Middlesex University Research Repository

An open access repository of

Middlesex University research

http://eprints.mdx.ac.uk

Copyright:

The item will be removed from the repository while any claim is being investigated.

See also repository copyright: re-use policy: http://eprints.mdx.ac.uk/policies.html#copy

Performance Analysis of Cooperative Transmission for Cognitive Wireless Relay Networks

Quoc-Tuan Vien, Huan X. Nguyen, Orhan Gemikonakli, Balbir Barn

School of Science and Technology, Middlesex University, The Burroughs, London NW4 4BT, UK.

Email: {q.vien; h.nguyen; o.gemikonakli; b.barn}@mdx.ac.uk

Abstract—In this paper, we consider cooperative transmission in cognitive wireless relay networks (CWRNs) over frequency-selective fading channels. We propose a new distributed space-time-frequency block code (DSTFBC) for a two-hop nonregenerative CWRN, where a primary source node and multiple secondary source nodes convey information data to their desired primary destination node and multiple secondary destination nodes via multiple cognitive relay nodes with dynamic spectrum access. The proposed DSTFBC is designed to achieve spatial diversity gain as well as allow for low-complexity decoupling detection at the receiver. Pairwise error probability is then analysed to study the achievable diversity gain of the proposed DSTFBC for different channel models including Rician fading and mixed Rayleigh-Rician fading.

I. INTRODUCTION

Cognitive radio (CR) has been an emerging technology proposed to improve spectrum efficiency by efficiently utilizing the available spectrum and exploiting the underutilised licensed spectrum [1]. Using dynamic spectrum access, spectrum holes can be opportunistically utilised by the secondary users (SUs) when the licensed primary users (PUs) are inactive. Recently, cooperative diversity has been incorporated into CR networks to construct a cognitive wireless relay network (CWRN) for seamless transmission by exploiting some portions of the spectrum not utilized by the PUs over a period of time [2]. Most of the literature on cooperative diversity for CWRNs has considered the transmission of either the PU or the SU over frequency-nonselective fading channels for low data-rate communications [2], [3]. However, in wide-band communication standards where the system is required to operate at a high data rate, multipath fading channels become frequency selective. These channels cause severe attenuation in signal strength and unreliable signal detection due to significant inter-symbol interference. In these environments, the cooperative transmission of both the PUs and SUs in a CWRN over frequency-selective fading channels for wide-band wireless communications has not previously been investigated. In addition, the diversity gain of cooperative communications in a CWRN for the general frequency-selective fading scenario where the cognitive relays are located either in the neighborhood of the sources or the destinations, or at the midpoint of the network has also been left unevaluated.

To provide a solution to these problems, in this paper, we design a new distributed space-time-frequency block code (DSTFBC) for two-hop CWRNs over frequency-selective fading channels using active cognitive relay nodes which employ the amplify-and-forward (AF) protocol. In order to facilitate the simultaneous data transmissions of all the PUs and SUs, spectrum access is firstly investigated to allocate the available frequency bands for the SUs. In our proposed DSTFBC, the cognitive relays help a PU and multiple SUs in the coverage of a CWRN to transmit their own data to their interested destinations. The main contributions of this paper can be summarized as follows:

- A precoding matrix at the cognitive relays is designed to allow decoupling detection of desired data blocks in both the time and frequency domains at $\mathcal{D}_0$ and also at $\{\mathcal{D}_1, \mathcal{D}_2, \ldots, \mathcal{D}_N\}$. This design facilitates the cooperative transmission of both the PU and the SUs over frequency-selective fading channels in CWRN context.
- The pairwise error probability (PEP) is analysed to study the achievable diversity gain of the proposed DSTFBC for a general scenario where the cognitive relays are located near either the sources or the destinations (in this case, channels between the relays and the sources/destinations are considered a mix of Rayleigh and Rician fading), or where the relays are at the centre of the network (i.e., channels are Rician).

The theoretical results demonstrate the achievable diversity order of our proposed scheme and show that the Rician fading factor in the line-of-sight (LOS) component provides a coding gain to the PEP performance. Additionally, through simulation results, our proposed DSTFBC scheme achieves a lower bit-error-rate (BER) when compared with the conventional interference cancellation scheme, resulting as a consequence of the achievable diversity gain of the proposed DSTFBC scheme.

Notation: Bold lower and upper case letters represent vectors and matrices, respectively; $(\cdot)^T$, $(\cdot)^*$ and $(\cdot)^{\mathcal{H}}$ denote transpose complex conjugate and Hermitian transpose, respectively; $E(\cdot)$, $\Phi(\cdot)$ and $f(\cdot)$ denote expectation value, moment generating and probability density functions, respectively; $[\mathbf{x}]_i$ and $[\mathbf{A}]_{i,j}$ represent i-th entry of vector $\mathbf{x}$ and (i, j)-th entry of matrix $\mathbf{A}$, respectively; $\|\mathbf{x}\|$ denotes Euclidean norm of vector $\mathbf{x}$; $\mathbf{B} = <\mathbf{A}>^2 \triangleq \mathbf{A}\mathbf{A}^{\mathcal{H}}$; $\mathbf{B} = \mathbf{A}^{1/2}$ represents a matrix $\mathbf{B}$ such that $\mathbf{B}^2 = \mathbf{A}$; $\otimes$ and $\oplus$ denote the matrix direct product and direct sum, respectively; $\mathbf{F}_M$ denotes the normalized $M \times M$ discrete Fourier transform (DFT) matrix where $[\mathbf{F}_M]_{m,n} = \frac{1}{\sqrt{M}}e^{-j2\pi(m-1)(n-1)/M}$ for all $1 \leq (m, n) \leq M$; $\mathbf{0}_{M \times N}$ and $\mathbf{I}_N$ denote the zero matrix of size $M \times N$ and the identity matrix of size $N \times N$, respectively.

II. SYSTEM MODEL, SPECTRUM ALLOCATION AND FADING CHANNEL MODEL

An overlay CWRN consisting of 2 PUs and N_s SUs is considered where the data transmissions of the PUs are at a higher priority. We assume there are K non-overlapping licensed frequency bands f_1, f_2, ..., f_K, in a wide-band channel. The two PUs can use either the whole or part of the wide-band channel to transmit data. Each SU transceiver is equipped with a software defined radio system to tune to any of the K licensed frequency band. The spectrum sensing process at a SU can be carried out using various spectrum sensing techniques (e.g. [4], [5]). A spectrum indicator vector (SIV) $\boldsymbol{\phi}_i$, $i = 1, 2, \ldots, N_s$, of length K (in bits) is used at the i-th SU to report the availability of frequency bands where bits '0' and '1' represent the frequency band being utilized by the PUs or available, respectively [5]. For example, following an energy detection rule for unknown signals over fading channels, the i-th SU, $i = 1, 2, \ldots, N_s$, can detect the usage of the k-th frequency band, $k = 1, 2, \ldots, K$, (i.e. $[\boldsymbol{\phi}_i]_k$). Accordingly, all SIVs at N_s SUs can be written in a spectrum indicator matrix (SIM) form as

$$\boldsymbol{\Phi} = \left[\boldsymbol{\phi}_1, \boldsymbol{\phi}_2, \ldots, \boldsymbol{\phi}_{N_s}\right]^T, \tag{1}$$

where $[\boldsymbol{\Phi}]_{i,k}$, $i = 1, 2, \ldots, N_s$, $k = 1, 2, \ldots, K$, represents the availability of the k-th frequency band for the i-th SU. It can be seen that the number of SUs that can communicate depends on the number of frequencies occupied by the PUs. Within CR framework, it is often considered that the states of available frequency can be modelled as a Markov chain where they evolve over time between idle and busy states [6]. However, within the scope of this work, we consider a specific sensing window where we can assume that there are N frequencies ($0 < N < K$) available for the N_s SUs. This means that there are a maximum of N pairs of SUs can communicate with each other using N available frequencies
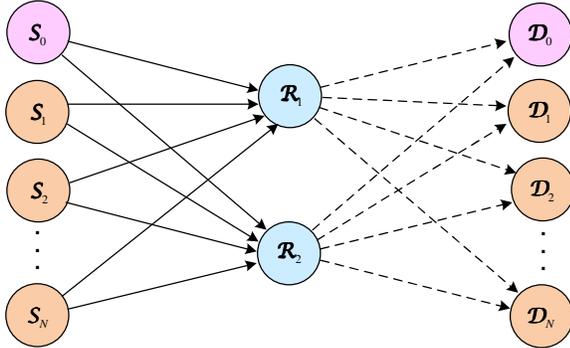

Fig. 1. System model of CWRN.

Therefore, as shown in Fig. 1, we investigate a specific two-relay CWRN with 1 PU source $\mathcal{S}_0$, 1 PU destination $\mathcal{D}_0$, N SU sources $\{\mathcal{S}_1, \mathcal{S}_2, \ldots, \mathcal{S}_N\}$, 2 SU relays $\{\mathcal{R}_1, \mathcal{R}_2\}$ and N SU destinations $\{\mathcal{D}_1, \mathcal{D}_2, \ldots, \mathcal{D}_N\}$. A half-duplex system is considered where all nodes can either transmit or receive data, but not concurrently. It is assumed that there are no direct links between any pair of source and destination nodes due to either power limitations in each node or distance between nodes or obstacles between nodes. The licensed band for the PU source and PU destination is assumed to be in the range $F_p = \{f_{p_1}, f_{p_2}, \ldots\} \in \{f_1, f_2, \ldots, f_K\}$. From (1), we can allocate the available frequency band $f_{s_i} \in F_s = \{f_1, f_2, \ldots, f_K\} \backslash F_p$, $i = 1, 2, \ldots, N$, for the i-th SU source and i-th SU destination based on the SIM.

In this paper, we take into consideration two typical fading models which include long-term and short-term fading. Specifically, we characterize long-term and short-term fading between two nodes $\mathcal{A}$ and $\mathcal{B}$, $\{\mathcal{A}, \mathcal{B}\} \in \{\mathcal{S}_0, \mathcal{S}_1, \mathcal{S}_2, \ldots, \mathcal{S}_N, \mathcal{D}_0, \mathcal{D}_1, \mathcal{D}_2, \ldots, \mathcal{D}_N, \mathcal{R}_1, \mathcal{R}_2\}$, by $\xi_{\mathcal{AB}}$ and $\mathbf{h}_{\mathcal{AB}}$, respectively. Here, $\mathbf{h}_{\mathcal{AB}} = [h_{\mathcal{AB}}(1), h_{\mathcal{AB}}(2), \ldots, h_{\mathcal{AB}}(L_{\mathcal{AB}})]^T$, where $L_{\mathcal{AB}}$ is the number of resolvable paths and $E[\|\mathbf{h}_{\mathcal{AB}}\|^2] = 1$.

III. PROPOSED DSTFBC FOR CWRNS AND PROOF OF DECOUPLING CAPABILITY

A. Proposed DSTFBC

In Fig. 1, each source transmits two data blocks to its interested destination through the assistance of two cognitive relays. Each transmitted data block $\mathbf{x}_{i,k}$, $i = 0, 1, 2, \ldots, N$, $k = 1, 2$, of length M_i is generated at $\mathcal{S}_i$ by adding a zero-padding (ZP) sequence ZP_i of length L_i to modulated information data block $\mathbf{s}_{i,j}$ of length B_i, which can be expressed as $\mathbf{x}_{i,j} = [\mathbf{s}_{i,j}^T, \mathbf{0}_{1 \times L_i}]^T$ where $\mathbf{s}_{i,j} = [[\mathbf{s}_{i,j}]_1, [\mathbf{s}_{i,j}]_2, \ldots, [\mathbf{s}_{i,j}]_{B_i}]^T$. To guarantee that the channel matrices $\mathcal{S}_i \rightarrow \mathcal{R}_1$, $\mathcal{S}_i \rightarrow \mathcal{R}_2$, $\mathcal{R}_1 \rightarrow \mathcal{D}_i$ and $\mathcal{R}_2 \rightarrow \mathcal{D}_i$ are circulant, the length of ZP_i must satisfy $L_i \geqslant \max(L_{\mathcal{S}_i \mathcal{R}_1} + L_{\mathcal{R}_1 \mathcal{D}_i}, L_{\mathcal{S}_i \mathcal{R}_2} + L_{\mathcal{R}_2 \mathcal{D}_i})$.

With proper allocation of available frequency bands $\{f_{s_1}, f_{s_2}, \ldots, f_{s_N}\}$ for all SU sources and destinations (see (1)), $\{\mathcal{S}_0, \mathcal{S}_1, \mathcal{S}_2, \ldots, \mathcal{S}_N\}$ simultaneously transmit two data blocks to both $\mathcal{R}_1$ and $\mathcal{R}_2$ in the first two time slots. $\mathcal{R}_1$ then amplifies and forwards its $(2N + 2)$ received signals to the destinations while $\mathcal{R}_2$ precodes its received signals by a precoding matrix before transmitting to all $\{\mathcal{D}_0, \mathcal{D}_1, \mathcal{D}_2, \ldots, \mathcal{D}_N\}$. The idea behind our design is that the precoding at $\mathcal{R}_2$ helps enable the decoupling detection of two desired data blocks at every destination.

We now present the data transmission and precoding process in our proposed DSTFBC for the CWRN. In the first two time slots, $\mathcal{S}_i$, $i = 0, 1, 2, \ldots, N$, serially transmits $\mathbf{x}_{i,k}$, $k = 1, 2$, to both $\mathcal{R}_1$ and $\mathcal{R}_2$ using its allocated frequency band f_i. The received signal at $\mathcal{R}_j$, $j = 1, 2$, from $\mathcal{S}_i$ is given by

$$\mathbf{r}_{i,k}^{(\mathcal{R}_j)} = \sqrt{\xi_{\mathcal{S}_i \mathcal{R}_j}} \mathbf{H}_{\mathcal{S}_i \mathcal{R}_j} \mathbf{x}_{i,k} + \boldsymbol{\eta}_{i,k}^{(\mathcal{R}_j)}, \tag{2}$$

where $\mathbf{H}_{\mathcal{S}_i \mathcal{R}_j}$ is an $M_i \times M_i$ circulant channel matrix and $\boldsymbol{\eta}_{i,k}^{(\mathcal{R}_j)}$ is a circularly symmetric complex Gaussian (CSCG) noise vector at $\mathcal{R}_j$ with each entry having zero-mean and variance of $N_0/2$ per dimension. It is noted that for any $M_{\mathcal{AB}} \times M_{\mathcal{AB}}$ circulant matrix $\mathbf{H}_{\mathcal{AB}}$, its (k, l)-th entry is written as $[\mathbf{H}_{\mathcal{AB}}]_{k,l} = [\mathbf{h}_{\mathcal{AB}}]_{((k-l+1) \bmod M_{\mathcal{AB}})}$.

What is unique in our proposed DSTFBC is that the received signal at $\mathcal{R}_2$ is conjugated and then precoded by a precoding matrix $\mathbf{P_R} \triangleq [[\mathbf{0}_{M \times M}, \mathbf{P}_M^{(G)}]^T, [-\mathbf{P}_M^{(G)}, \mathbf{0}_{M \times M}]^T]$ where

$\mathbf{P}_M^{(G)} \triangleq \mathbf{P}_1 \oplus \mathbf{P}_2$. Here, $\mathbf{P}_1$ and $\mathbf{P}_2$ are binary matrices of size $G \times G$ and $(M-G) \times (M-G)$, respectively, where $[\mathbf{P}_1]_{l,k} = 1$ if $k = G - l + 1$ and $[\mathbf{P}_2]_{l,k} = 1$ if $k = M - G - l + 1$. In order to ensure that, after precoding, at least the last $L_{\mathcal{S}_i \mathcal{R}_2}$, $i = 0, 1, 2, \ldots, N$, samples of $-\mathbf{P}_M^{(G)} \mathbf{r}_{i,2}^{'(\mathcal{R}_2)}$ and $\mathbf{P}_M^{(G)} \mathbf{r}_{i,1}^{'(\mathcal{R}_2)}$ are all zeros to make the channel matrix $\mathcal{R}_2 \to \mathcal{D}_i$ circulant, we choose $G = \max(B_0, B_1, B_2, \ldots, B_N) + \max(L_{\mathcal{S}_0 \mathcal{R}_2}, L_{\mathcal{S}_1 \mathcal{R}_2}, L_{\mathcal{S}_2 \mathcal{R}_2}, \ldots, L_{\mathcal{S}_N \mathcal{R}_2})$. The proposed precoding matrix is specifically designed to assist the cooperative data transmission of the PU and SUs in CWRNs.

Subsequently, each cognitive relay $\mathcal{R}_j$, $j = 1, 2$, normalizes its received signal $\mathbf{r}_{i,k}^{(\mathcal{R}_j)}$, $i = 0, 1, 2, \ldots, N$, $k = 1, 2$, in (2) by a factor $\alpha_i^{(\mathcal{R}_j)} = \sqrt{E[\|\mathbf{r}_{i,k}^{(\mathcal{R}_j)}\|^2]} = \sqrt{\xi_{\mathcal{S}_i \mathcal{R}_j} + N_0}$ to have unit average energy. Then, $\mathcal{R}_1$ and $\mathcal{R}_2$ simultaneously forward their messages to $\{\mathcal{D}_0, \mathcal{D}_1, \mathcal{D}_2, \ldots, \mathcal{D}_N\}$ using $\{F_p, f_{s_1}, f_{s_2}, \ldots, f_{s_N}\}$ in the subsequent $(2N+2)$ time slots. The received signals at $\mathcal{D}_i$, $i = 0, 1, 2, \ldots, N$, are therefore given by

$$\mathbf{r}_k^{(\mathcal{D}_i)} = \frac{\sqrt{\xi_{\mathcal{R}_1 \mathcal{D}_i}}}{\alpha_i^{(\mathcal{R}_1)}} \mathbf{H}_{\mathcal{R}_1 \mathcal{D}_i} \mathbf{r}_{i,k}^{'(\mathcal{R}_1)} \\ + (-1)^k \frac{\sqrt{\xi_{\mathcal{R}_2 \mathcal{D}_i}}}{\alpha_i^{(\mathcal{R}_2)}} \mathbf{H}_{\mathcal{R}_2 \mathcal{D}_i} \mathbf{P}_M^{(G)} [\mathbf{r}_{i,\bar{k}}^{'(\mathcal{R}_2)}]^* + \boldsymbol{\eta}_k^{(\mathcal{D}_i)}, \quad (3)$$

where $k = 1, 2$, $\bar{k} = 3 - k$, $\mathbf{H}_{\mathcal{R}_j \mathcal{D}_i}$, $j = 1, 2$, is an $M \times M$ circulant channel matrix and $\boldsymbol{\eta}_k^{(\mathcal{D}_i)}$ is a CSCG noise vector at $\mathcal{D}_i$ with each entry having zero-mean and variance of $N_0/2$ per dimension.

B. Decoupling in Time and Frequency Domains

For the sake of a fair comparison with other systems, we firstly normalize the noise variance of the received signals at $\mathcal{D}_i$, $i = 0, 1, 2, \ldots, N$, in (3) to be N_0 by a factor $\left(\frac{\xi_{\mathcal{R}_1 \mathcal{D}_i}}{\xi_{\mathcal{S}_i \mathcal{R}_1} + N_0} \sum_{l=1}^{L_{\mathcal{R}_1 \mathcal{D}_i}} \left|[\mathbf{h}_{\mathcal{R}_1 \mathcal{D}_i}]_l\right|^2 + \frac{\xi_{\mathcal{R}_2 \mathcal{D}_i}}{\xi_{\mathcal{S}_i \mathcal{R}_2} + N_0} \sum_{l=1}^{L_{\mathcal{R}_2 \mathcal{D}_i}} \left|[\mathbf{h}_{\mathcal{R}_2 \mathcal{D}_i}]_l\right|^2 + 1\right)^{1/2}$. Accordingly, the normalized signal at $\mathcal{D}_i$ can be written as

$$\mathbf{r}_k^{'(\mathcal{D}_i)} = \alpha_{i,1} \mathbf{H}_{\mathcal{R}_1 \mathcal{D}_i} \mathbf{H}_{\mathcal{S}_i \mathcal{R}_1} \mathbf{x}_{i,k} \\ + (-1)^k \alpha_{i,2} \mathbf{H}_{\mathcal{R}_2 \mathcal{D}_i} \mathbf{P}_M^{(G)} \mathbf{H}_{\mathcal{S}_i \mathcal{R}_2}^* \mathbf{x}_{i,\bar{k}}^* + \boldsymbol{\eta}_k^{''(\mathcal{D}_i)}, \quad (4)$$

where $k = 1, 2$, $\bar{k} = 3 - k$ and $\boldsymbol{\eta}_k^{''(\mathcal{D}_i)}$ is a normalized CSCG noise vector in which each entry has zero mean and variance of $N_0/2$ per dimension. Here, $\alpha_{i,j} \triangleq$

$$\sqrt{\frac{\alpha_{i,n \neq j}' \alpha_{i,j}'' \xi_{\mathcal{S}_i \mathcal{R}_j}}{\alpha_{i,1}' \alpha_{i,2}' + \alpha_{i,2}' \alpha_{i,1}'' \sum_{l=1}^{L_{\mathcal{R}_1 \mathcal{D}_i}} \left|[\mathbf{h}_{\mathcal{R}_1 \mathcal{D}_i}]_l\right|^2 + \alpha_{i,1}' \alpha_{i,2}'' \sum_{l=1}^{L_{\mathcal{R}_2 \mathcal{D}_i}} \left|[\mathbf{h}_{\mathcal{R}_2 \mathcal{D}_i}]_l\right|^2}},$$

where $i = 0, 1, 2, \ldots, N$, $j = 1, 2$, $n = 1, 2$, $\alpha_{i,j}' = 1 + \xi_{\mathcal{S}_i \mathcal{R}_j}/N_0$ and $\alpha_{i,j}'' = \xi_{\mathcal{R}_j \mathcal{D}_i}/N_0$.

For data decoupling, we conjugate both sides of (4) with $k = 2$ and then multiply with $\mathbf{P}_M^{(G)}$. Based on the fact that $\mathbf{P}_M^{(G)} \mathbf{H}_{\mathcal{A}\mathcal{B}}^* \mathbf{P}_M^{(G)} = \mathbf{H}_{\mathcal{A}\mathcal{B}}^{\mathcal{H}}$ for any $M \times M$ circulant matrix $\mathbf{H}_{\mathcal{A}\mathcal{B}}$, we obtain

$$\mathbf{r}_2^{''(\mathcal{D}_i)} = \alpha_{i,2} \mathbf{H}_{\mathcal{R}_2 \mathcal{D}_i}^{\mathcal{H}} \mathbf{H}_{\mathcal{S}_i \mathcal{R}_2} \mathbf{x}_{i,1} \\ + \alpha_{i,1} \mathbf{H}_{\mathcal{R}_1 \mathcal{D}_i}^{\mathcal{H}} \mathbf{H}_{\mathcal{S}_i \mathcal{R}_1}^{\mathcal{H}} \mathbf{P}_M^{(G)} \mathbf{x}_{i,2}^* + \mathbf{P}_M^{(G)} [\boldsymbol{\eta}_2^{''(\mathcal{D}_i)}]^*. \quad (5)$$

From (4) with $k = 1$ and (5), we can group the equations as

$$\mathbf{R}^{(\mathcal{D}_i)} = \begin{bmatrix} \mathbf{r}_1^{'(\mathcal{D}_i)} \\ \mathbf{r}_2^{''(\mathcal{D}_i)} \end{bmatrix} = \mathbf{H}_i \begin{bmatrix} \mathbf{x}_{i,1} \\ \mathbf{P}_M^{(G)} \mathbf{x}_{i,2}^* \end{bmatrix} + \begin{bmatrix} \boldsymbol{\eta}_1^{''(\mathcal{D}_i)} \\ \mathbf{P}_M^{(G)} [\boldsymbol{\eta}_2^{''(\mathcal{D}_i)}]^* \end{bmatrix}, \quad (6)$$

where

$$\mathbf{H}_i \triangleq \begin{bmatrix} \alpha_{i,1} \mathbf{H}_{\mathcal{R}_1 \mathcal{D}_i} \mathbf{H}_{\mathcal{S}_i \mathcal{R}_1} & -\alpha_{i,2} \mathbf{H}_{\mathcal{R}_2 \mathcal{D}_i} \mathbf{H}_{\mathcal{S}_i \mathcal{R}_2}^{\mathcal{H}} \\ \alpha_{i,2} \mathbf{H}_{\mathcal{R}_2 \mathcal{D}_i}^{\mathcal{H}} \mathbf{H}_{\mathcal{S}_i \mathcal{R}_2} & \alpha_{i,1} \mathbf{H}_{\mathcal{R}_1 \mathcal{D}_i}^{\mathcal{H}} \mathbf{H}_{\mathcal{S}_i \mathcal{R}_1}^{\mathcal{H}} \end{bmatrix}. \quad (7)$$

Let us denote $\boldsymbol{\Omega}_i = [\alpha_{i,1}^2 <\mathbf{H}_{\mathcal{S}_i \mathcal{R}_1}>^2 <\mathbf{H}_{\mathcal{R}_1 \mathcal{D}_i}>^2 + \alpha_{i,2}^2 <\mathbf{H}_{\mathcal{S}_i \mathcal{R}_2}>^2 <\mathbf{H}_{\mathcal{R}_2 \mathcal{D}_i}>^2]^{\frac{1}{2}}$. Then, $\mathbf{H}_i^{\mathcal{H}} \mathbf{H}_i = \mathbf{I}_2 \otimes \boldsymbol{\Omega}_i^2$, which is a block-diagonal matrix. Thus, we can decouple the detection of two data blocks independently by multiplying both sides of (6) with unitary matrix $(\mathbf{I}_2 \otimes \boldsymbol{\Omega}_i^{-1}) \mathbf{H}_i^{\mathcal{H}}$. Two data blocks transmitted from $\mathcal{S}_i$, $i = 0, 1, 2, \ldots, N$, can be detected independently at $\mathcal{D}_i$ by using general maximum likelihood (ML) detection in the time domain. However, general ML detection requires high computational complexity at the destinations.

It is noted that the circulant matrix $\mathbf{H}_{\mathcal{A}\mathcal{B}}$ of size $M \times M$ can be diagonalized as $\mathbf{H}_{\mathcal{A}\mathcal{B}} = \mathbf{F}_M^{\mathcal{H}} \boldsymbol{\Lambda}_{\mathcal{A}\mathcal{B}} \mathbf{F}_M$ where $\boldsymbol{\Lambda}_{\mathcal{A}\mathcal{B}}$ is an $M \times M$ diagonal matrix with diagonal entries created by the M-point DFT of the first column of $\mathbf{H}_{\mathcal{A}\mathcal{B}}$. Thus, we can transform (6) into the frequency domain by taking the DFT of both sides of the equation, which results in

$$\mathbf{R}_f^{(\mathcal{D}_i)} = \boldsymbol{\Lambda}_i \begin{bmatrix} \mathbf{F}_M \mathbf{x}_{i,1} \\ \mathbf{F}_M \mathbf{P}_M^{(G)} \mathbf{x}_{i,2}^* \end{bmatrix} + \begin{bmatrix} \mathbf{F}_M \boldsymbol{\eta}_1^{''(\mathcal{D}_i)} \\ \mathbf{F}_M \mathbf{P}_M^{(G)} [\boldsymbol{\eta}_2^{''(\mathcal{D}_i)}]^* \end{bmatrix}, \quad (8)$$

where

$$\boldsymbol{\Lambda}_i \triangleq \begin{bmatrix} \alpha_{i,1} \boldsymbol{\Lambda}_{\mathcal{R}_1 \mathcal{D}_i} \boldsymbol{\Lambda}_{\mathcal{S}_i \mathcal{R}_1} & -\alpha_{i,2} \boldsymbol{\Lambda}_{\mathcal{R}_2 \mathcal{D}_i} \boldsymbol{\Lambda}_{\mathcal{S}_i \mathcal{R}_2}^* \\ \alpha_{i,2} \boldsymbol{\Lambda}_{\mathcal{R}_2 \mathcal{D}_i}^* \boldsymbol{\Lambda}_{\mathcal{S}_i \mathcal{R}_2} & \alpha_{i,1} \boldsymbol{\Lambda}_{\mathcal{R}_1 \mathcal{D}_i}^* \boldsymbol{\Lambda}_{\mathcal{S}_i \mathcal{R}_1}^* \end{bmatrix}. \quad (9)$$

Let us denote $\boldsymbol{\Psi}_i = [\alpha_{i,1}^2 <\boldsymbol{\Lambda}_{\mathcal{S}_i \mathcal{R}_1}>^2 <\boldsymbol{\Lambda}_{\mathcal{R}_1 \mathcal{D}_i}>^2 + \alpha_{i,2}^2 <\boldsymbol{\Lambda}_{\mathcal{S}_i \mathcal{R}_2}>^2 <\boldsymbol{\Lambda}_{\mathcal{R}_2 \mathcal{D}_i}>^2]^{\frac{1}{2}}$. We observe that $\boldsymbol{\Lambda}_i^{\mathcal{H}} \boldsymbol{\Lambda}_i = \mathbf{I}_2 \otimes \boldsymbol{\Psi}_i^2$, which is a block-diagonal matrix. Thus, by multiplying both sides of (8) with the unitary matrix $(\mathbf{I}_2 \otimes \boldsymbol{\Psi}_i^{-1}) \boldsymbol{\Lambda}_i^{\mathcal{H}}$, we can decouple the detection of each data block at $\mathcal{D}_i$, $i = 0, 1, 2, \ldots, N$, in the frequency domain as follows:

$$\mathbf{Y}_f^{(\mathcal{D}_i)} = \begin{bmatrix} \mathbf{y}_{f,1}^{(\mathcal{D}_i)} \\ \mathbf{y}_{f,2}^{(\mathcal{D}_i)} \end{bmatrix} = \begin{bmatrix} \boldsymbol{\Psi}_i \mathbf{F}_M \mathbf{x}_{i,1} \\ \boldsymbol{\Psi}_i \mathbf{F}_M \mathbf{P}_M^{(G)} \mathbf{x}_{i,2}^* \end{bmatrix} + \begin{bmatrix} \bar{\boldsymbol{\eta}}_{f,1}^{(\mathcal{D}_i)} \\ \bar{\boldsymbol{\eta}}_{f,2}^{(\mathcal{D}_i)} \end{bmatrix}, \quad (10)$$

where $\bar{\boldsymbol{\eta}}_{f,k}^{(\mathcal{D}_i)}$, $k = 1, 2$, is the equivalent noise vector for the k-block at $\mathcal{D}_i$ resulting from the decoupling process in the frequency domain. Since $\boldsymbol{\Psi}_i$ is diagonal, we can decompose (10) into scalar equations and transform the evaluated outputs into the time domain to detect $[\mathbf{x}_{i,k}]_n$, $k = 1, 2$, accordingly.

IV. PERFORMANCE ANALYSIS

In this section, we derive the PEP expression of the proposed DSTFBC scheme for CWRNs over three typical scenarios of frequency selective fading channels as follows:

(a) The cognitive relays are located near the sources.
(b) The cognitive relays are located near the destinations.
(c) The cognitive relays are located near the midpoint in the network.

It can be seen that the PEP expression for scenario (b) can be obtained simply from scenario (a) with some interchanged parameters. Thus, it is sufficient to analyse the PEP for scenarios (a) and (c).

Let us denote a decoded codeword vector at $\mathcal{D}_i$, $i = 0, 1, 2, \ldots, N$, as $\hat{\mathbf{x}}_i$. The conditional PEP is upper bounded by

$$P(\mathbf{x}_i \to \hat{\mathbf{x}}_i) = Q\left(\sqrt{\frac{d^2(\mathbf{x}_i, \hat{\mathbf{x}}_i)}{2N_0}}\right) \leqslant \exp\left(-\frac{d^2(\mathbf{x}_i, \hat{\mathbf{x}}_i)}{4N_0}\right), \quad (11)$$

where $d(\mathbf{x}_i, \hat{\mathbf{x}}_i)$ is the Euclidean distance between $\mathbf{x}_i$ and $\hat{\mathbf{x}}_i$, which is calculated by

$$d^2(\mathbf{x}_i, \hat{\mathbf{x}}_i) = \alpha_{i,1}^2 \|\mathbf{H}_{\mathcal{R}_1 \mathcal{D}_i} \mathbf{H}_{\mathcal{S}_i \mathcal{R}_1}(\mathbf{x}_{i,1} - \hat{\mathbf{x}}_{i,1})\|^2$$
$$+ \alpha_{i,2}^2 \|\mathbf{H}_{\mathcal{R}_2 \mathcal{D}_i} \mathbf{H}_{\mathcal{S}_i \mathcal{R}_2} \mathbf{P}_M^{(G)}(\mathbf{x}_{i,2} - \hat{\mathbf{x}}_{i,2})\|^2. \quad (12)$$

In (12), each component of the summations of the right hand side can be expressed by either one of the two following factors

$$d_1^2 = \sum_{l_{\mathcal{R}_k \mathcal{D}_i} = 1}^{L_{\mathcal{R}_k \mathcal{D}_i}} |[\mathbf{h}_{\mathcal{R}_k \mathcal{D}_i}]_{l_{\mathcal{R}_k \mathcal{D}_i}}|^2 \sum_{l_{\mathcal{S}_i \mathcal{R}_k} = 1}^{L_{\mathcal{S}_i \mathcal{R}_k}} [\boldsymbol{\lambda}_k]_{l_{\mathcal{S}_i \mathcal{R}_k}} |[\boldsymbol{\nu}_k]_{l_{\mathcal{S}_i \mathcal{R}_k}}|^2, \quad (13)$$

$$d_2^2 = \sum_{l_{\mathcal{S}_i \mathcal{R}_k} = 1}^{L_{\mathcal{S}_i \mathcal{R}_k}} |[\mathbf{h}_{\mathcal{S}_i \mathcal{R}_k}]_{l_{\mathcal{S}_i \mathcal{R}_k}}|^2 \sum_{l_{\mathcal{R}_k \mathcal{D}_i} = 1}^{L_{\mathcal{R}_k \mathcal{D}_i}} [\boldsymbol{\lambda}_k]_{l_{\mathcal{R}_k \mathcal{D}_i}} |[\boldsymbol{\nu}_k]_{l_{\mathcal{R}_k \mathcal{D}_i}}|^2, \quad (14)$$

where $[\boldsymbol{\lambda}_k]_{l_{\mathcal{AB}}}$ and $\boldsymbol{\nu}_k$ denote the eigenvalue of the codeword difference matrix and the zero-mean complex Gaussian vector with unit variance, respectively.

For simplicity of mathematical formulation, let us denote $L_{\mathcal{S}_i \mathcal{R}_k} = L_1$, $L_{\mathcal{R}_k \mathcal{D}_i} = L_2$, $\mathbf{h}_{\mathcal{S}_i \mathcal{R}_k} = \mathbf{h}_1$ and $\mathbf{h}_{\mathcal{R}_k \mathcal{D}_i} = \mathbf{h}_2$. The PEP will now be analysed for scenarios (a) and (c).

A. Scenario (a): $\mathcal{S}_i \to \{\mathcal{R}_1, \mathcal{R}_2\}$: Rician fading, $\{\mathcal{R}_1, \mathcal{R}_2\} \to \mathcal{D}_i$: Rayleigh fading

Due to the different characteristics of fading channels, there are three situations based on the relationship of L_1 and L_2.

1) Case 1 ($L_1 < L_2$): Eq. (13) is taken into consideration. Let us define $Z_1 = d_1^2 = X_1 Y_1$ where $X_1 = \sum_{l_2=1}^{L_2} |[\mathbf{h}_2]_{l_2}|^2$ and $Y_1 = \sum_{l_1=1}^{L_1} [\boldsymbol{\lambda}]_{l_1} |[\boldsymbol{\nu}]_{l_1}|^2$. Applying the Chernoff bound, the PEP corresponding to d_1^2 is upper bounded by $E_{Z_1}[\exp(-\alpha^2 Z_1/4N_0)] = \Phi_{Z_1}(s)|_{s=-\alpha^2/4N_0}$. Here, α corresponds to α_k, $k = 1, 2$, if we consider $\mathcal{R}_k$, and $\Phi_{Z_1}(s)$ can be evaluated as [7]

$$\Phi_{Z_1}(s) = \int_0^\infty f_{X_1}(x_1) \Phi_{Y_1}(sx_1) dx_1, \quad (15)$$

where $f_{X_1}(x_1) = \frac{L_2^{L_2}}{\Gamma(L_2)} \frac{x_1^{L_2-1}}{e^{L_2 x_1}}$ and $\Phi_{Y_1}(s) = \prod_{l_1=1}^{L_1} \frac{1+n^2}{1+n^2-s[\boldsymbol{\lambda}]_{l_1}} e^{\frac{n^2 s[\boldsymbol{\lambda}]_{l_1}}{1+n^2-s[\boldsymbol{\lambda}]_{l_1}}}$. Here n is the Nakagami-n or Rician fading parameter and $\Gamma(\cdot)$ represents the Gamma

function [8]. Assuming high signal-to-noise ratio (SNR), i.e. $\alpha^2/4N_0 \gg 1$, and $(1+n^2)/n^2 \approx 1$, (15) can be approximated as

$$\Phi_{Z_1}(s)|_{s=-\frac{\alpha^2}{4N_0}} \approx \left[\frac{L_2(1+n^2)}{e^{n^2}}\right]^{L_1} \frac{\Gamma(L_2-L_1)}{\Gamma(L_2)}$$
$$\times \left(\frac{\alpha^2}{4N_0}\right)^{-L_1} \prod_{l_1=1}^{L_1} \frac{1}{[\boldsymbol{\lambda}]_{l_1}}. \quad (16)$$

2) Case 2 ($L_1 > L_2$): Let us examine (14) and define $Z_2 = d_2^2 = X_2 Y_2$ where $X_2 = \sum_{l_1=1}^{L_1} |[\mathbf{h}_1]_{l_1}|^2$ and $Y_2 = \sum_{l_2=1}^{L_2} [\boldsymbol{\lambda}]_{l_2} |[\boldsymbol{\nu}]_{l_2}|^2$. Similarly, applying the Chernoff bound, the PEP corresponding to d_2^2 is upper bounded by $E_{Z_2}[\exp(-\alpha^2 Z_2/4N_0)] = \Phi_{Z_2}(s)|_{s=-\alpha^2/4N_0}$ where

$$\Phi_{Z_2}(s) = \int_0^\infty f_{X_2}(x_2) \Phi_{Y_2}(sx_2) dx_2. \quad (17)$$

Here $f_{X_2}(x_2) = \frac{L_1^{\frac{3-L_1}{2}}}{n^{L_1-1}} \frac{x_2^{\frac{L_1-1}{2}} I_{L_1-1}[2L_1^{\frac{3}{2}} n x_2^{\frac{1}{2}}]}{e^{L_1^2 n^2 + L_1 x_2}}$ and $\Phi_{Y_2}(s) = \prod_{l_2=1}^{L_2} \frac{1}{1-s[\boldsymbol{\lambda}]_{l_2}}$. where $I_\alpha(\beta)$ denotes the modified Bessel function of the first kind [8]. Under the assumption of high SNR (i.e. $\alpha^2/4N_0 \gg 1$), (17) can be approximated as

$$\Phi_{Z_2}(s)|_{s=-\frac{\alpha^2}{4N_0}} \approx \frac{L_1^{L_2} \Gamma(L_1-L_2)}{e^{L_1^2 n^2}} {}_1\tilde{F}_1(L_1-L_2; L_1; L_1^2 n^2)$$
$$\times \left(\frac{\alpha^2}{4N_0}\right)^{-L_2} \prod_{l_2=1}^{L_2} \frac{1}{[\boldsymbol{\lambda}]_{l_2}}, \quad (18)$$

where ${}_1\tilde{F}_1(a; b; z)$ is the regularized hypergeometric function defined as ${}_1\tilde{F}_1(a; b; z) \triangleq \frac{1}{\Gamma(a)} \sum_{k=0}^\infty \frac{\Gamma(a+k)}{\Gamma(b+k)} \frac{z^k}{k!}$ [8].

3) Case 3 ($L_1 = L_2$): Let us consider (13), for which

$$\Phi_{Z_1}(s)|_{s=-\frac{\alpha^2}{4N_0}} = \frac{L_1^{L_1}(1+n^2)^{L_1}}{\Gamma(L_1) e^{L_1 n^2}} \left(\frac{\alpha^2}{4N_0}\right)^{-L_1}$$
$$\times \prod_{l_1=1}^{L_1} \frac{1}{[\boldsymbol{\lambda}]_{l_1}} \int_0^\infty \frac{x_1^{L_1-1} e^{-L_1(1+n^2)x_1}}{\prod_{l_1=1}^{L_1}\left(x_1 + \frac{1}{\frac{\alpha^2}{4N_0}[\boldsymbol{\lambda}]_{l_1}}\right)} dx_1. \quad (19)$$

By using some mathematical calculations [8], we obtain

$$\Phi_{Z_1}(s)|_{s=-\frac{\alpha^2}{4N_0}} = \left[\frac{L_1(1+n^2)}{e^{n^2}}\right]^{L_1} \left(\frac{\alpha^2}{4N_0}\right)^{-L_1}$$
$$\times \sum_{l_1=1}^{L_1} \frac{p_{l_1}}{[\boldsymbol{\lambda}]_{l_1}^{L_1}} e^{\frac{L_1(n^2+1)}{\frac{\alpha^2}{4N_0}[\boldsymbol{\lambda}]_{l_1}}} \Gamma\left[1-L_1, \frac{L_1(n^2+1)}{\frac{\alpha^2}{4N_0}[\boldsymbol{\lambda}]_{l_1}}\right], \quad (20)$$

where $p_{l_1} \triangleq \prod_{l=1, l \neq l_1}^{L_1} \frac{[\boldsymbol{\lambda}]_{l_1}}{[\boldsymbol{\lambda}]_{l_1} - [\boldsymbol{\lambda}]_l}$ and $\Gamma[\alpha, x]$ is the incomplete Gamma function defined by $\Gamma[\alpha, x] \triangleq \int_x^\infty t^{\alpha-1} e^{-t} dt$ [8].

B. Scenario (c): $\mathcal{S}_i \to \{\mathcal{R}_1, \mathcal{R}_2\}$ and $\{\mathcal{R}_1, \mathcal{R}_2\} \to \mathcal{D}_i$: Rician fading

Let n_1 and n_2 denote the Rician fading parameters of the links $\mathcal{S}_i \to \{\mathcal{R}_1, \mathcal{R}_2\}$ and $\{\mathcal{R}_1, \mathcal{R}_2\} \to \mathcal{D}_i$, respectively. Similarly, we investigate three cases as follows:

1) Case 1 ($L_1 < L_2$): We also take into consideration (13) and evaluate $\Phi_{Z_1}(s)$ where

$$f_{X_1}(x_1) = \frac{L_2^{\frac{3-L_2}{2}} x_1^{\frac{L_2-1}{2}} I_{L_2-1}[2L_2^{\frac{3}{2}} n_2 x_1^{\frac{1}{2}}]}{n_2^{L_2-1} e^{L_2^2 n_2^2 + L_2 x_1}}, \qquad (21)$$

$$\Phi_{Y_1}(s) = \prod_{l_1=1}^{L_1} \frac{1+n_1^2}{1+n_1^2 - s[\boldsymbol{\lambda}]_{l_1}} e^{\frac{n_1^2 s[\boldsymbol{\lambda}]_{l_1}}{1+n_1^2 - s[\boldsymbol{\lambda}]_{l_1}}}. \qquad (22)$$

Substituting (21) and (22) into (15) under high SNR, we obtain

$$\Phi_{Z_1}(s)\big|_{s=-\frac{\alpha^2}{4N_0}} \approx \frac{[L_2(1+n_1^2)]^{L_1}}{e^{L_2^2 n_2^2 + L_1 n_1^2}} \Gamma(L_2 - L_1)$$
$$\times {}_1\tilde{F}_1\left(L_2 - L_1; L_2; L_2^2 n_2^2\right) \left(\frac{\alpha^2}{4N_0}\right)^{-L_1} \prod_{l_1=1}^{L_1} \frac{1}{[\boldsymbol{\lambda}]_{l_1}}. \qquad (23)$$

2) Case 2 ($L_1 > L_2$): By considering (14) with the same approach as Case 1, $\Phi_{Z_2}(s)\big|_{s=-\frac{\alpha^2}{4N_0}}$ can be approximated by

$$\Phi_{Z_2}(s)\big|_{s=-\frac{\alpha^2}{4N_0}} \approx \frac{[L_1(1+n_2^2)]^{L_2}}{e^{L_1^2 n_1^2 + L_2 n_2^2}} \Gamma(L_1 - L_2)$$
$$\times {}_1\tilde{F}_1\left(L_1 - L_2; L_1; L_1^2 n_1^2\right) \left(\frac{\alpha^2}{4N_0}\right)^{-L_2} \prod_{l_2=1}^{L_2} \frac{1}{[\boldsymbol{\lambda}]_{l_2}}. \qquad (24)$$

3) Case 3 ($L_1 = L_2$): Similarly, with some mathematical calculations [8], we obtain

$$\Phi_{Z_1}(s)\big|_{s=-\frac{\alpha^2}{4N_0}} = \frac{L_1^{3-2L_1}}{e^{L_1^2 n_2^2 + L_1 n_1^2}} \frac{1+n_1^2}{n_2^{2L_1-2}} \left(\frac{\alpha^2}{4N_0}\right)^{-L_1}$$
$$\times \sum_{l_1=1}^{L_1} \frac{p_{l_1}}{[\boldsymbol{\lambda}]_{l_1}} \left[\Gamma(L_1-1, -L_1^2 n_2^2) - \Gamma(L_1-1)\right]. \qquad (25)$$

From the PEP analysis of fading scenario (a) with Eqs. (16), (18) and (20) and fading scenario (c) with Eqs. (23), (24) and (25), we can conclude that the diversity gain of our proposed DSTFBC for both the primary and secondary transmissions in all three fading scenarios is $\min(L_{\mathcal{S}_i\mathcal{R}_1}, L_{\mathcal{R}_1\mathcal{D}_i}) + \min(L_{\mathcal{S}_i\mathcal{R}_2}, L_{\mathcal{R}_2\mathcal{D}_i})$, $i = 0, 1, 2, \ldots, N$, by observing the exponential terms of $\frac{\alpha^2}{4N_0}$. Additionally, it can be observed that the Rician fading parameters do not produce any diversity gain, however, they play a similar function to coding gain, and thus can improve the PEP.

V. Simulation Results

In this section, we evaluate the uncoded BER performance of the proposed DSTFBC in a CWRN to confirm the analysis of the achievable diversity gain over either mixed Rayleigh-Rician fading channels or both Rayleigh or Rician fading channels. The validity of our analysis can be confirmed through the slope of the BER curves since BER is proportional to PEP. The simulation is carried out in MATLAB using quadrature phase shift keying (QPSK) modulation with Gray mapping and each transmitted data block consists of 256 symbols including the zero sequence and modulated information data. We consider a uniform power delay profile and a quasi-static
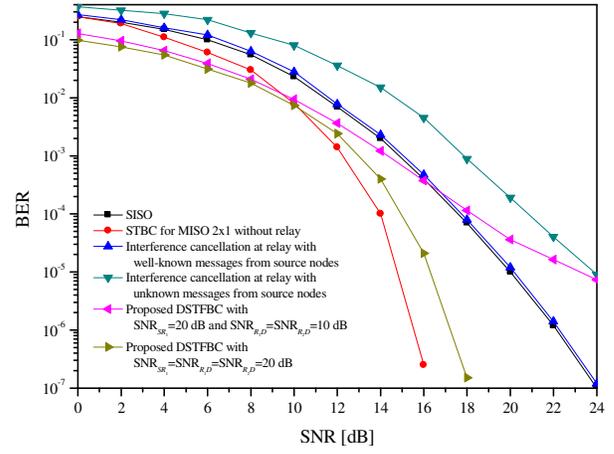

Fig. 2. Performance comparison of various transmission schemes in a CWRN.

fading channel model with perfect channel state information at the destinations.

Fig. 2 shows the BER performance comparison of the primary transmission using the proposed DSTFBC, and compares it with the following schemes: single-input single-output (SISO), space-time block code (STBC) and interference cancelation at the cognitive relay (ICR). The fading of links $\mathcal{S}_0 \rightarrow \{\mathcal{R}_1, \mathcal{R}_2\}$ and $\{\mathcal{R}_1, \mathcal{R}_2\} \rightarrow \mathcal{D}_0$ are assumed to be frequency-selective Rayleigh fading where the channel memory lengths are $L_{\mathcal{S}_0\mathcal{R}_1} = 5$, $L_{\mathcal{S}_0\mathcal{R}_2} = 7$, $L_{\mathcal{R}_1\mathcal{D}_0} = 5$, $L_{\mathcal{R}_2\mathcal{D}_0} = 7$. We assume that the value of $\xi_{\mathcal{S}_0\mathcal{R}_1}/N_0$ is fixed at 20 dB and $\xi_{\mathcal{R}_1\mathcal{D}_0} = \xi_{\mathcal{R}_2\mathcal{D}_0} = \xi_{\mathcal{R}\mathcal{D}_0}$. The STBC scheme refers to the classical 2×1 STBC where each path from one antenna of $\mathcal{S}_0$ to $\mathcal{D}_0$ has 6 taps (i.e. $L_{\mathcal{S}_0\mathcal{D}_0} = 6$). The ICR scheme refers to the scheme where the cognitive relay helps the primary and secondary users decode, precode and forward their messages to the respective primary and secondary receivers using a precoding scheme at the cognitive relay for interference compensation. In Fig. 2, SNR is referred to $\xi_{\mathcal{S}_0\mathcal{D}_0}/N_0$ for the direct transmission scenario without relay assistance, while SNR is referred to $\xi_{\mathcal{S}_0\mathcal{R}_2}/N_0$ for the relaying scenario. It can be observed that the ICR scheme with unknown messages from the sources shows the worst performance. The SISO and ICR systems perform better than the DSTFBC in the high-SNR region due to the existence of an error floor when $\xi_{\mathcal{R}\mathcal{D}_0}$ is small. At high $\xi_{\mathcal{R}\mathcal{D}_0}/N_0$, the BER performance curves of the DSTFBC and conventional STBC schemes have the same slope, reflecting the same diversity order. As proved in the PEP analysis, the diversity gain of our proposed DSTFBC for the primary transmission is $\min(L_{\mathcal{S}_0\mathcal{R}_1}, L_{\mathcal{R}_1\mathcal{D}_0}) + \min(L_{\mathcal{S}_0\mathcal{R}_2}, L_{\mathcal{R}_2\mathcal{D}_0}) = 12$, which is also the maximum diversity gain of $(2 \times L_{\mathcal{S}_0\mathcal{D}_0}) = 12$ achieved with STBC.

Fig. 3 shows the BER performances of the first secondary transmissions over Rayleigh fading as a function of $\xi_{\mathcal{S}_1\mathcal{R}_2}/N_0$ using the proposed DSTFBC for various combinations of channel lengths. We assume that $\xi_{\mathcal{S}_0\mathcal{R}_1}/N_0 = 20$ dB, $\xi_{\mathcal{S}_1\mathcal{R}_1}/N_0 = 15$ dB, $\xi_{\mathcal{R}_1\mathcal{D}_0} = \xi_{\mathcal{R}_2\mathcal{D}_0} = \xi_{\mathcal{R}\mathcal{D}_0} = 10$ dB and
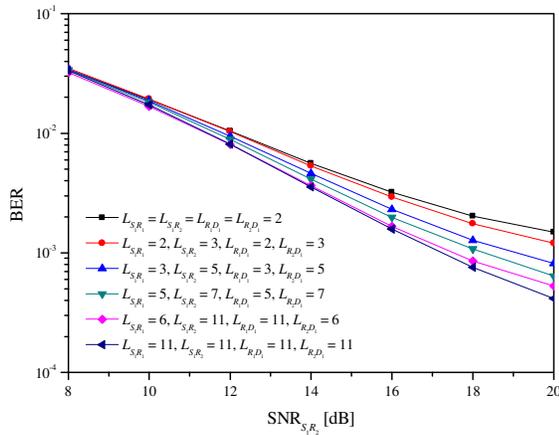
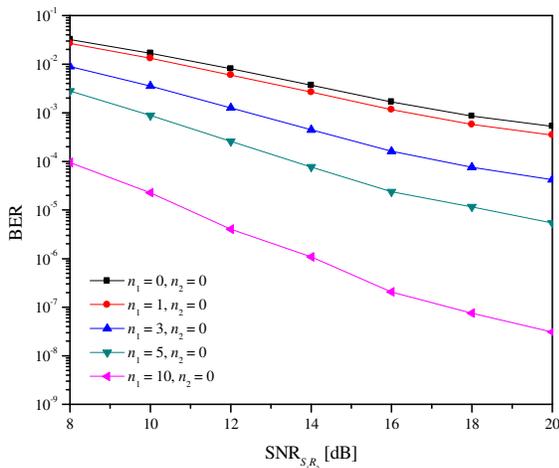Fig. 3.   BER of SU transmission over Rayleigh fading.

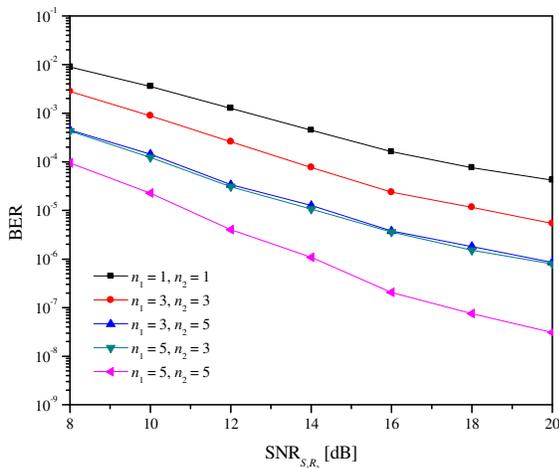Fig. 4.   BER of SU transmission over mixed Rician-Rayleigh fading.

Fig. 5.   BER of SU transmission over Rician fading.

$\xi_{\mathcal{R}_1\mathcal{D}_1} = \xi_{\mathcal{R}_2\mathcal{D}_1} = \xi_{\mathcal{R}\mathcal{D}_1} = 5$ dB. It can be observed that the diversity gain is improved with increasing number of channel memory taps, which results in steeper BER curves.

The performance of the proposed DSTFBC for the secondary transmissions over wireless fading channels where

the cognitive relays are located near the sources and near the midpoint is shown in Figs. 4 and 5, respectively. The performance of the proposed DSTFBC for the scenario where the cognitive relays are located near the destinations can be similarly observed, and thus it has been omitted for simplicity. The channel memory orders of fading channels $\{\mathcal{S}_1\} \rightarrow \{\mathcal{R}_1, \mathcal{R}_2\}$ and $\{\mathcal{R}_1, \mathcal{R}_2\} \rightarrow \mathcal{D}_1$ are assumed to be $L_{\mathcal{S}_1\mathcal{R}_1} = 6$, $L_{\mathcal{S}_1\mathcal{R}_2} = 11$, $L_{\mathcal{R}_1\mathcal{D}_1} = 11$, $L_{\mathcal{R}_2\mathcal{D}_1} = 6$. The BER performances of the secondary transmissions are plotted as a function of $\xi_{\mathcal{S}_1\mathcal{R}_2}/N_0$ with different values of Rician fading factor n_1 and n_2. Here, n_1 and n_2 denote the Rician fading parameters of the links $\mathcal{S}_1 \rightarrow \{\mathcal{R}_1, \mathcal{R}_2\}$ and $\{\mathcal{R}_1, \mathcal{R}_2\} \rightarrow \mathcal{D}_1$, respectively. The SNR values of the other links are similarly set as in Fig. 3. It can be seen that improved performance is achieved as either n_1 or n_2 increases. However, the slopes of the BER curves are almost the same at high SNR, which means that they achieve the same diversity gain. This can be explained as the influence of the LOS component on the BER gain through all ranges of SNR values where the Rician fading parameter only produces coding gain to the BER as we can see in the analysis. This also confirms our conclusion about the achievable diversity gain which is independent of the Rician fading factor.

VI. CONCLUSIONS

In this paper, a new DSTFBC scheme for two-hop CWRNs over frequency-selective fading channels has been proposed. The proposed DSTFBC can achieve a spatial diversity order of $\min(L_{\mathcal{S}_i\mathcal{R}_1}, L_{\mathcal{R}_1\mathcal{D}_i}) + \min(L_{\mathcal{S}_i\mathcal{R}_2}, L_{\mathcal{R}_2\mathcal{D}_i})$, $i = 0, 1, 2, \ldots, N$, for both primary and secondary transmissions, and a low-complexity decoupling at destinations. Furthermore, the PEP performance has been analyzed for various scenarios of cognitive relay location. The analysis and simulation results have validated the theoretically derived diversity order and have shown that the LOS component in Rician fading effectively improves the error rate performance at the destinations.

REFERENCES

[1] J. Wang, M. Ghosh, and K. Challapali, "Emerging cognitive radio applications: A survey," *IEEE Commun. Mag.*, vol. 49, no. 3, pp. 74–81, Mar. 2011.

[2] K. Ben Letaief and W. Zhang, "Cooperative communications for cognitive radio networks," *Proc. of the IEEE*, vol. 97, no. 5, pp. 878–893, May 2009.

[3] M. Sarkar, T. Ratnarajah, and M. Sellathurai, "Outage performance of MIMO multiple access interference channel with cognitive relay," in *Proc. IEEE ICC 2010*, Cape Town, South Africa, May 2010, pp. 1–5.

[4] T. Yucek and H. Arslan, "A survey of spectrum sensing algorithms for cognitive radio applications," *IEEE Commun. Surveys and Tutorials*, vol. 11, no. 1, pp. 116–130, first quarter 2009.

[5] Q.-T. Vien, H. Tianfield, and B. G. Stewart, "Efficient cooperative spectrum sensing for cognitive wireless relay networks over Rayleigh flat fading channels," in *Proc. IEEE VTC 2012-Spring*, Yokohama, Japan, May 2012, pp. 1–5.

[6] X. Ma, S. Djouadi, and H. Li, "State estimation over a semi-Markov model based cognitive radio system," *IEEE Trans. Wireless Commun.*, vol. 11, no. 7, pp. 2391–2401, Jul. 2012.

[7] A. Stuart and J. K. Ord, *Kendall's advanced theory of statistics*, 5th ed. C. Griffin, London, U.K., 1987.

[8] I. S. Gradshteyn and I. M. Ryzhik, *Table of Integrals, Series, and Products*, 7th ed.   Academic Press, 2007.